IAC-19-F1.2.3

Improvements in BepiColombo and JUICE radio science experiments with a multi-station tracking configuration for the reduction of Doppler noise

A. Di Ruscio[a]*, P. Cappuccio[a], V. Notaro[a], M. Di Benedetto[a]

[a] *Department of Mechanical and Aerospace Engineering, Sapienza University of Rome, via Eudossiana 18, Roma, 00184*, Italy
* Corresponding Author. Tel.: +39 06 4458 5976. E-mail: andrea.diruscio@uniroma1.it

Abstract

Radio science experiments for planetary geodesy mostly rely on measurements of the Doppler shift of microwave signals sent to a spacecraft by an Earth station, and retransmitted back coherently in phase to the same antenna (two-way link). The retransmitted signal can also be received by a different station in a listen-only configuration (three-way link). In state-of-the-art tracking systems, such as the ones will be used on the future ESA's missions JUICE and BepiColombo, the Doppler error budget is dominated by local noise sources arising at the ground-station, in particular tropospheric scintillation and unmodeled motions of the antenna's structure. In this work, a novel technique aimed at reducing these disturbances is analyzed, with particular emphasis on its benefits to BepiColombo's and JUICE's radio science experiments. The method, referred to as Time-Delay Mechanical-noise Cancellation (TDMC), relies on simultaneous two-way and three-way spacecraft tracking, the latter employing a stiffer listen-only antenna with better mechanical stability and located in a favorable dry region more immune to tropospheric noise. In fact, a proper linear combination of time-shifted observables from the two-way and three-way links can replace local noises of the two-way ground-station with those coming from the listen-only antenna, translating into increased accuracy of the final measurements, while preserving the original Doppler content. We show the results of covariance analyses performed with a multi-arc weighted least square estimator for the entire BepiColombo's Hermean phase and JUICE's flybys of Callisto. We compare the two solutions obtained with and without the application of the TDMC technique. For BepiColombo and JUICE radio science experiments, the two-way links are baselined from the 35-m DSA-3 (Malargüe, Argentina) and the 34-m DSS 25 (Goldstone, California). For the three-way link, we select the 12-m Large Latin American Millimeter Array (LLAMA) antenna for three reasons: 1) its mechanical rigidity with respect to large beam-waveguide antennas , 2) its unique position in the extremely dry Puna de Atacama desert, that assures low tropospheric noise, and 3) its limited longitudinal separation from the two other ground-stations, granting sufficient common visibility time to perform the requested combination of the observables. Besides its noise-reduction effect, enabling unprecedented levels of accuracy on Doppler measurements, TDMC provides also a back-up for unique events: a crucial satellite flyby or a specific passage over a site of particular geophysical interest. Indeed, measurements become virtually independent of unfavorable meteorological conditions at the transmitting station.

Keywords: (maximum 6 keywords)

Nomenclature

σ	ADEV
τ	Integration time
$\mathcal{T}$	RTLT
f	Fourier frequency
y	Doppler frequency fluctuations
S_y	PSD
M	Antenna mechanical noise
T	Tropospheric scintillation noise
C	FTS noise
$*_2$	Two-way link relative terms
$*_3$	Three-way link relative terms

Acronyms/Abbreviations

3GM	Gravity and Geophysics of Jupiter and Galilean Moons
ADEV	Allan Deviation
APEX	Atacama Pathfinder Experiment
CA	Closest Approach
CSO	Cryogenic Sapphire Oscillator
DSA	Deep Space Antenna
DSN	Deep Space Network
DSS	Deep Space Station
DST	Deep Space Transponder
ESO	European Southern Observatory
FTS	Frequency and Timing System
GS	Ground-Station
HAA	High Accuracy Accelerometer
HGA	High Gain Antenna
ISA	Italian Spring Accelerometer
JAXA	Japanese Aerospace Exploration Agency
JUICE	Jupiter Icy Moons Explorer

KaT	Ka-band Transponder
LLAMA	Large Latin American Millimeter Array
MGA	Medium Gain Antenna
MMO	Mercury Magnetospheric Orbiter
MORE	Mercury Orbiter Radio Science Experiment
MPO	Mercury Planetary Orbiter
PSD	Power Spectral Density
PWV	Precipitable Water Vapor
RMS	Root Mean Square
RTLT	Round-Trip Light-Time
SC	Space-Craft
TDMC	Time-Delay Mechanical Noise Cancellation
TT&C	Telemetry, Tracking and Command
ZWD	Zenith Wet Delay

1. Introduction

Radio science approach to planetary geodesy consists in determining the state of a SC orbiting a celestial body, while solving for a series of physical parameters of interest, such as its gravity field coefficients, tidal Love numbers, rotational state, etc. Radio signals sent to the satellite and coherently retransmitted at the GS are used in the process. In a two-way link configuration the same transmitting GS is used to receive the downlink signal as well, while in a three-way a second listen-only antenna is used as receiver (Fig. 1). Typically, Doppler measurements are adopted, providing for a measure of the relative motion between the SC and the GS expressed via Doppler shift on the reference frequency of the radio signal carrier.

The precision of these observables directly affects the level of accuracy achievable in the estimation of the parameters, hence, a precise description of the error budget becomes fundamental in assessing radio science experiments results. The most adopted Doppler noise characterization in time-domain is the Allan deviation [1], defined as

$$\sigma(\tau) = \sqrt{\frac{1}{2(M-1)}\sum_{i=1}^{M-1}(y_{i+1}-y_i)^2} \qquad (1)$$

where y_i is the i-th of M fractional frequency values averaged over the sampling interval τ.

State-of-the-art radio science experiments rely on multi-frequency links that permit the almost complete cancellation of dispersive noise, i.e. solar and ionospheric plasma fluctuations. The noise budget is then dominated by local noises arising in the proximity of the GS, such as tropospheric scintillation and mechanical noise introduced by the antenna structure [2].

Deep space antennas present indeed notable sizes, with parabolic dishes ranging from 34 to 70 m in diameter, and are subject to thermal expansions, gravity loadings and wind gusts throughout the tracking passages, introducing relevant disturbances on the measurements; typical values are $\sigma \approx 1.6 \times 10^{-14}$ or 0.005 mm/s at τ=60s [3].

Tropospheric noise refers to the frequency/phase fluctuations introduced on the signal along its propagation path in the Earth's atmosphere. If its dry component contributing to almost the 90% of the path delay can be effectively calibrated, it is the hardly predictable wet part that afflicts the frequency stability most. This noise is related to the weather conditions and the amount of water vapor in the air at the GS, therefore it presents significant seasonal variations, with measured peaks of $\sigma \approx 10^{-13}$ at τ=60s [3].

Even if considerably smaller, instabilities introduced by the GS FTS represent another important disturbance to the link. Modern Hydrogen-Maser clocks installed at DSN's and ESA's stations provide $\sigma \approx 10^{-15}$ at 1000s, with a dominant white frequency noise behavior ($\sigma \propto \tau^{-1/2}$) at lower integration times, 10-1000s. Hopefully their short-term stability can be improved with the adoption of CSOs as the one installed at DSS 25, assuring $\sigma \approx 10^{-15}$ even at τ <100s [4].

The different noise contributions appear in the Doppler link through their respective transfer-functions, based on their nature and specific configuration of the link. Two-way link, for example, introduces a characteristic modulation in the power spectrum of local noises

$$h_2(t) = \delta(t) \pm \delta(t-\mathcal{T}) \qquad (2)$$

The same antenna is in fact used both to transmit and to receive the signal, hence, all those noises arising at the GS will echo in the downlink after a RTLT. Tropospheric and mechanical disturbances introduce a positive correlation ($+\delta(t-\mathcal{T})$) while clock jitters are anticorrelated ($-\delta(t-\mathcal{T})$).

In 2008 Armstrong et al. [5] showed that this characteristic can be exploited by suitably combining simultaneous two- and three-way measurements, in order to suppress tropospheric and mechanical noise from the two-way GS, reducing significantly the Doppler link instability.

In this paper, an assessment of the possible advantages achievable by adopting this technique on modern and near-future interplanetary missions is presented. In particular, covariance analysis results for

the next ESA BepiColombo's MORE and JUICE's 3GM radio science experiments are provided.

The work is structured as follows: in section 2 a description of the noise-reduction technique referred to as TDMC is provided. Section 3 briefly introduces the missions, BepiColombo and JUICE, on which the technique has been tested. Section 4 presents the methodology adopted for the analysis and the models used in the simulations. Simulations results are discussed in section 5 while conclusive thoughts are expressed in section 6.

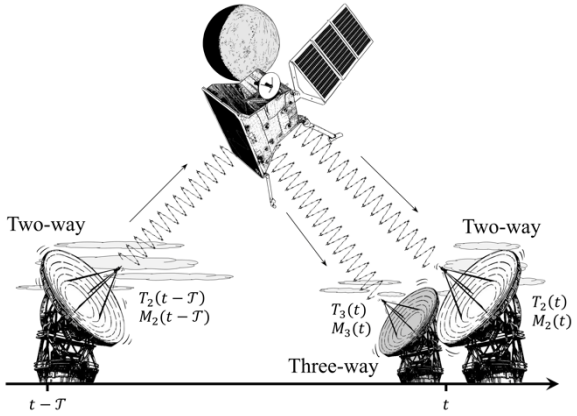

Figure 1. Sketch depicting two-way and three-way link configuration for BepiColombo mission. Local noise contributions arising at transmitting $(t-\mathcal{T})$ and receiving (t) times are shown for the two stations. The uplink is sent by the two-way station a RTLT before the downlink signal is received-back by the same antenna and the three-way one.

2. Time-Delay Mechanical-Noise Cancellation

A technique to reduce tropospheric scintillation and antenna mechanical noise has been first proposed by Armstrong et al. [5] along with a proof-of-concept that successfully demonstrated its feasibility. The aim is to mitigate GS local disturbances by exploiting their characteristic modulation in the two-way and three-way links. Doppler frequency fluctuations can be schematized as follows, by neglecting lower order noise sources

$$y_2(t) = M_2(t) + M_2(t-\mathcal{T}) + T_2(t) + T_2(t-\mathcal{T}) + C_2(t) - C_2(t-\mathcal{T}) + y_S(t) \quad (2)$$

$$y_3(t) = M_3(t) + M_2(t-\mathcal{T}) + T_3(t) + T_2(t-\mathcal{T}) + C_3(t) - C_2(t-\mathcal{T}) + y_S(t) \quad (3)$$

where $y_S(t)$ is the two-way Doppler signal corrected for the GS motion.

In this formulation, the modulation introduced by the link configuration on the signals (Eq. 2) is evident; in particular, how the echoes of the two-way GS local noises participate in both links. It is thus possible to combine the two signals as follows

$$E(t) = y_3(t) + y_3(t-\mathcal{T}) - y_2(t-\mathcal{T}) = \quad (4)$$

$$= M_3(t) + M_3(t-\mathcal{T}) + T_3(t) + T_3(t-\mathcal{T}) + C_3(t) + C_3(t-\mathcal{T}) - 2C_2(t-\mathcal{T}) + y_S(t) \quad (5)$$

As result of the combination, the new observable $E(t)$ resembles in its structure a fictitious two-way link carried-out by the listen-only antenna, operating both as transmitter and receiver, while preserving the original Doppler content y_S. Indeed, the M_2 and T_2 terms are cancelled, or rather replaced by their three-way antenna counterparts. This substitution represents the key element to the noise reduction process; in fact, the measurements are now virtually independent from the main antenna, whose mechanical stability is limited by its size, and its location is forced to be chosen between the few deep space complexes in visibility. The choice of a smaller and stiffer listen-only antenna, then, located in a favourable dry location, allows a potential order-of-magnitude enhancement of the measurements accuracy, achieving an abrupt reduction of local noises. As downside the GS clock noise is doubled

Between many candidates to ancillary antenna, the most promising results to be LLAMA, a 12-m astronomic antenna still under construction, located in the arid desert of Puna de Atacama in Argentina, one of the driest place on Earth, at an altitude of 4,820 m.

The antenna is provided by Vertex, the same company who built the near APEX, and they share the same characteristics. Analyses [6] conducted on APEX showed a factor of 10 greater mechanical stability with respect to DSS 25, due to the limited dimension of the dish and the rigidity and low thermal expansion coefficients of the adopted materials.

Moreover, a thorough characterization of Atacama troposphere has been conducted over the years by ESO with water-vapor radiometers [7], showing order-of-magnitude improvements over DSN's Goldstone complex [8] under favourable conditions (austral winter).

3. MORE and 3GM

3.1 BepiColombo's MORE experiment

BepiColombo will be the first European mission to visit Mercury after NASA's Mariner 10 (1974) and MESSENGER (2011). Launched in October 2018, it consists of two separate SCs that will study the innermost planet of the solar system from two different orbits: ESA's MPO, that will analyze Mercury from an inner polar orbit (480×1,500 km) and JAXA's MMO, which

will remain on a larger eccentricity orbit (590×11,640 km), focusing on Mercury's magnetosphere study.

BepiColombo's radio science experiment MORE will feature a wide range of measures, from heliophysics and fundamental physics to Mercury's geodesy [9] [10]. In particular the gravity experiment will estimate Mercury's gravity field spherical harmonic coefficients up to degree and order 50, tidal Love number k_2 and its pole direction and librations. The experiment will rely on the most advanced telecommunication system ever flown on an interplanetary mission, involving multiple instruments: beside the GS, the DST used for TT&C, the steerable HGA and the KaT [11]. The latter is the scientific payload and represents the key element of MORE; capable of receiving and coherently retransmitting in Ka-band, it enables the almost complete calibration of dispersive noise, making de facto the observables independent from the solar elongation angle [3]. The cutting-edge accuracy of the measurements will then be limited by GS local noises, making BepiColombo the optimal candidate to benefit from TDMC capabilities. MORE will be supported by the accelerometer ISA, which will measure, and thus calibrate, all the non-gravitational accelerations acting on the SC.

MPO will start its nominal mission around Mercury on march 2026, and will orbit the planet for one year, with a possible extension of another year. During this period daily tracking from Earth will grant continuous data coverage. The nominal tracking configuration for MORE will consist of multi-link (X/X, X/Ka, Ka/Ka) two-way Doppler and Range data collected from ESA's DSA-3 (Malargüe, Argentina), following a X-band navigation passage from one of the ESA's stations in visibility.

The orbit will follow a natural evolution, with no manoeuvres foreseen except for the desaturation ones. Two reaction-wheel desaturations per day are scheduled, with the first one occurring during the navigation passage and the second one out of the tracking windows.

3.2 JUICE's 3GM experiment

The Jupiter Icy Moon Explorer is an ESA mission to Jupiter focused on the study of three Galilean Moons of the gas giant: Ganymede, Europa and Callisto. Expected to launch in June 2022, it will enter in Jupiter's orbit in 2030, and, after 3.5 years touring the Jovian system, will spend 9 months orbiting Ganymede, being the first SC to ever orbit a satellite out of our Moon.

During the orbital tour, JUICE will perform 2 gravity flybys of Europa, sufficient to understand whether the body is in a hydrostatic equilibrium ($J_2/C_{22}=10/3$) or not, and 12 flybys of Callisto, measuring its gravity field (at least 3×3) and Love number k_2. Measurements of Callisto's tidal response are crucial in order to infer the presence of a liquid ocean beneath the icy shell of the moon [12].

Similarly to MORE, 3GM measurements will benefit of the HAA accelerometer data to calibrate undesired accelerations acting on the SC, while the onboard KaT will grant multi-link Doppler and range data, providing for the cancellation of plasma scintillation noise.

During the moons flybys, the SC will be Nadir pointed with the HGA and the other instruments directed towards the moons; hence, 3GM radio link will be established with the steerable MGA of JUICE.

JUICE's flybys will be tracked 2 days before and after each CA with the moon from the ESA stations in visibility, assuming that Ka-band receivers will be installed on all the three complexes (Malargüe, Cebreros and New Norcia) before the mission start.

4. Methodology

4.1 Covariance analyses

In order to assess the benefits of TDMC on the parameters estimate, a covariance analysis has been conducted, based on complete simulations of the two experiments, 3GM and MORE (section 3.1 and 3.2).

The analyses consist of two separate steps, a simulation process aimed at replicating the measurements that will be gathered by the SC (*observed* observables), and an estimation process during which synthetic measurements based on a first-guess dynamical model are generated (*computed* observables) along with the residuals vector (*observed* - *computed* observables). The latter is then processed in a weighted least square filter (the in-house developed ORACLE), in an iterative process aimed at estimating the best values of the state-vector that minimize the residuals [13].

In a pure covariance analysis the same model used to generate the *observed* observables in the simulation is used in the estimation process as well; hence, the a priori values coincide with the simulated ones and iterating is not required.

A multi-arc strategy [14] has been adopted in the analyses. The method consists in dividing the trajectory in shorter arcs (365 arcs of 24h for BepiColombo and 12 arcs, one for each flybys of Callisto, for JUICE) in order to avoid filter divergency and numerical issues. The state vector is then divided in two categories: *local* parameters, i.e. the parameters pertinent to the single arc (SC state, manoeuvres, etc.) and *global* parameters, comprising the constant values common to all the arcs (planet's *GM*, spherical harmonics, Love number k_2, etc.).

4.2 Dynamical models and solve-for parameters

4.2.1 BepiColombo

BepiColombo's setup used in the simulations includes 50×50 gravity field of Mercury based on MESSENGER's HgM005 solution [15], point mass gravity perturbations from all the other planets with the *GM* and oblateness of the Sun. General relativity effects,

solar radiation pressure and desaturation manoeuvres are accounted as well.

For the orbits of the planets and the Moon INPOP17a ephemerides are used.

The adjusted parameters comprise the SC state vector and the $\Delta\mathbf{V}$ of the desaturation manoeuvres as *local* parameters; Mercury's gravity field up to degree and order 50, k_2 and planet's rotational state as *global* ones. In addition, calibration coefficients of ISA's low-frequency (planet's orbital period) and high-frequency (MPO's orbital period) error are estimated respectively as *local* and *global* parameters.

4.2.2 JUICE

The dynamical model of JUICE's flybys simulations includes Callisto's gravity field inferred from Galileo data [16], the gravity field of Europa, Ganymede, Jupiter and the *GM* of all the planets and the Sun.

The estimated *local* parameters are limited to JUICE's state, while the *global* vector comprises Callisto's ephemerides, 5×5 gravity field harmonic coefficients, k_2 and the HAA bias and bias-rate calibration parameters.

Table 1. Noise model used in the simulations. The one-way power-laws spectral densities modelling the different noise sources are presented; for local disturbances both DSA-3 and LLAMA antennas contributions are reported.

Noise source	$S_y(f)$ (One-way, two-sided)[Hz^{-1}]
M_2(DSA-3)	$10^{-30}f^{-1} + 5 \times 10^{-26}f^{1/3}$
M_3 (LLAMA)	$10^{-32}f^{-1} + 5 \times 10^{-28}f^{1/3}$
T_2 (DSA-3, winter)	$1.3 \times 10^{-26}f^{-1/3}$
T_2 (DSA-3, summer)	$6.7 \times 10^{-26}f^{-1/3}$
T_3 (LLAMA)	ESO Radiometers data [7]
$C_2 = C_3$ (H-Maser)	$1.5 \times 10^{-28} + 2 \times 10^{-26}f + 9 \times 10^{-32}f^{-1}$
GS Rcvr$_2$ (DSA-3)	$10^{-24}f^2$
GS Rcvr$_3$ (LLAMA)	$7 \times 10^{-24}f^2$
KaT+DST	$2.5 \times 10^{-25}f$
HGA mech. BepiColombo	4×10^{-27}
MGA mech. JUICE	1.5×10^{-27}

4.3 Noise modelling

In order to properly replicate real data, simulated noise is added to the generated *observed* observables. Noise simulation (Tab. 1) is based on Notaro et al. [17] model. This has been readapted for the specific analysis

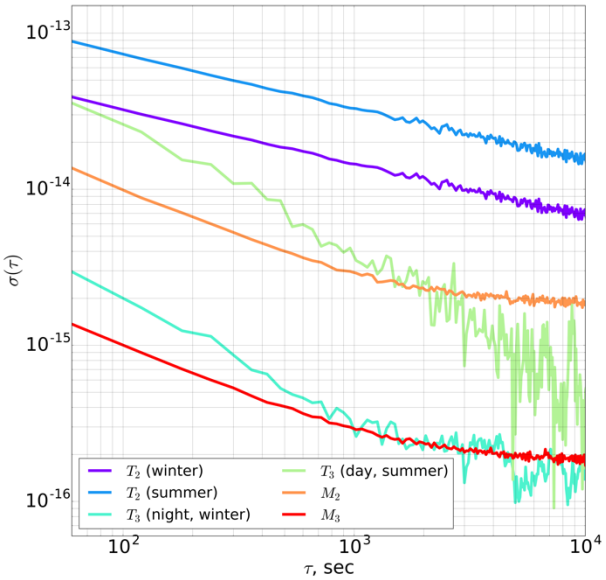

Figure 2. ADEV of simulated local noises for the two stations. Best (night, austral winter) and worst (day, summer) cases are depicted for tropospheric scintillation at LLAMA. The extremely dry troposphere of Atacama provides a factor of 20 amelioration in wintert ime conditions. Moreover, an order-of-magnitude increasing in mechanical stability is registered for the 12-m antenna with respect to typical deep space antennas values.

of BepiColombo's orbital phase and JUICE's flybys of Callisto.

Since TDMC relies on the modulation of PSDs of determined noise sources, a specific frequency characterization of each disturbance is mandatory. A widely adopted approach to characterize colored random fluctuations is to use power-law spectral densities

$$S_y(f) = \sum h_\alpha f^\alpha \qquad (6)$$

Once PSDs of noise sources are defined, it is possible to generate N^{th} order time-series for each of them, with a chosen sampling time Δ_t. In fact, by generating a random phase realization ϕ_j, the discrete Fourier-transformed signal can be computed as

$$\begin{aligned} \tilde{y}(f_j) &= \sqrt{S_y(f_j)\frac{N}{\Delta_t}}e^{i\phi_j}, \text{ for } j = 0, \dots, \left(\frac{N}{2} - 1\right) \\ \tilde{y}(f_j) &= \sqrt{S_y(f_j)\frac{N}{\Delta_t}}e^{-i\phi_j}, \text{ for } j = \frac{N}{2}, \dots, N \end{aligned} \qquad (7)$$

with $f_j = \frac{j}{N\Delta_t}$, and thus, the time-series y(t) is obtained with the inverse discrete Fourier transform

$$\tilde{y}(f_j) \xrightarrow{\mathcal{F}^{-1}} y(\Delta_t) \tag{8}$$

The generated one-way terms are then summed as shown in Eq. 2 and Eq. 3 to produce respectively the two-way and three-way total contributions.

Differently from the other noise sources, LLAMA's tropospheric scintillation, is retrieved directly from water-vapor radiometer measurements. In fact, the ESO's weather station installed in the Chajnantor Plateau of the Atacama desert provides for PWV data among other information, and its historical archive has public access [7]. From PWV, it is possible to retrieve ZWD due to the wet contribution of tropospheric scintillation as follows

$$ZWD(t) = \frac{PWV(t)}{\Pi} \tag{9}$$

with typical values for Π of ~0.16 [18].

By neglecting the elevation term, ZWD translates directly into phase variations and consequently frequency fluctuations of the signal

$$x(t) = \frac{\phi(t)}{2\pi f_0} = \frac{ZWD(t)}{c} \tag{10}$$

$$T_3(t) = y(t) = \frac{1}{2\pi f_0}\frac{d\phi(t)}{dt} = \frac{dx(t)}{dt} \tag{11}$$

The timeseries retrieved from weather station data highlight strong seasonal and diurnal variations of PWV, with higher variability in summer daytime. These trends reflect on the results of TDMC, and in particular are visible on the RMS of residuals, since both missions present year-long datasets. With this in mind, winter (from May to October) and summer (from November to April) periods have been identified, and two different noise levels have been chosen for simulating the respective arcs' noise (Fig. 2).

5. Results and Discussion

A comparison of the formal uncertainties achieved in the simulations using a two-way tracking configuration and with the application of TDMC are reported, for both the gravity experiment of BepiColombo's Hermean phase and JUICE's flybys of Callisto. Due to the large number of estimated parameters, only the uncertainties of the *GM*, J_2 and k_2 of Mercury and Callisto are shown. For MORE, results on the estimate of Mercury's rotational state are reported as well.

5.1 Results on MORE gravity experiment

As result of the application of TDMC on BepiColombo's gravity experiment, a general enhancement of ~40% on the estimate of gravity coefficients is registered. In particular a gain of 1.6 is observed on the estimate of Mercury's *GM* and 1.7 for J_2 and k_2 (Tab. 2). Moreover, the same level of amelioration registered on J_2 is measured on the higher degree coefficients of gravity field as well. This means that the adoption of TDMC could provide an higher resolution of MORE's gravity field estimate, enabling refined analyses of the planet's crust structures.

For what concerns Mercury's rotational state, gains factor of ~1.7 are achieved on the estimate of RA and Dec of the pole and the longitudinal librations, potentially providing tighter constraints on the interior structure of the planet.

The enhancements on the positioning of the SC with respect to the planet are depicted in Fig. 3. Since the SC state vector is a *local* parameter, it is more affected by the diurnal and seasonal variations simulated for the tropospheric noise at the GSs and this is clearly visible in the oscillations of the gain factors depicted in the right-most plots (blue lines). However, an overall gain factor of ~2 is observed, producing precious benefits for all those instruments whose measurements rely on a precise knowledge of the SC position, e. g. the BELA altimeter.

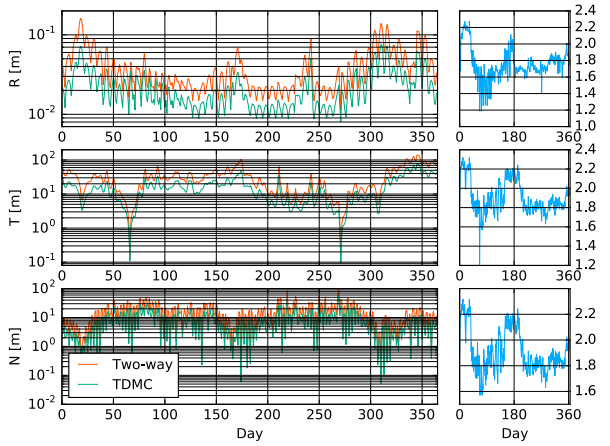

Figure 3. MPO's position formal accuracies in the Mercury-centered Radial-Transverse-Normal frame, obtained with the nominal two-way tracking configuration and with the use of TDMC. The blue lines on the right show the respective gain factors registered on the three components.

Table 2. Results of BepiColombo's MORE covariance-analysis. In particular formal uncertainties for Mercury's *GM*, J_2, Love number and rotational state are reported for both the reference two-way and the TDMC-enhanced solutions.

GM [km³/s²]	J_2	k_2	*RA* [arcsec]	*Dec* [arcsec]	*Lib* [arcsec]
Two-way (DSA 3):					
2.1E-4	7.4E-11	5.2E-4	0.53	0.18	0.35
TDMC (DSA 3 / LLAMA):					
3.3E-4	4.3E-11	5.2E-4	0.29	0.11	0.20

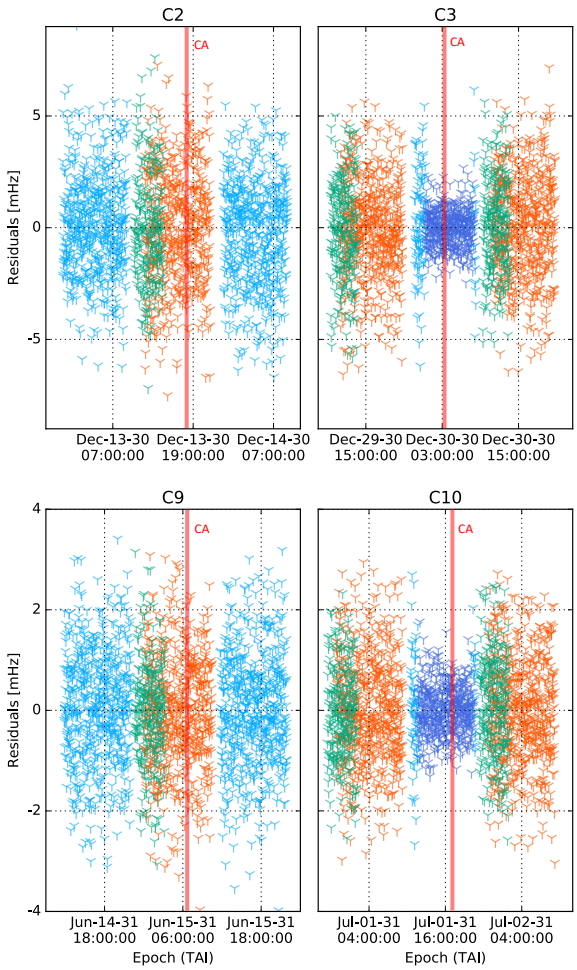

Figure 4. Residuals for JUICE's flybys of Callisto C2, C3 (austral summer), C9 and C10 (winter). On C3 and C10, TDMC is applied on the CA tracking passage, registering respectively ~2 and 2.5 times smaller RMS. The residuals highlight how the technique is more efficient in summertime, when tropospheric contribution on the link instability is dominant, and thus its suppression leads to a greater reduction of the overall Doppler noise.

5.2 Results on Callisto's flybys of JUICE

The application of TDMC on 3GM's Doppler data results in an overall reduction of a factor >2 on the RMS of the residuals (Fig. 4). However, the current predicted orbit shows that not all CA passages will be tracked from DSA 3. At this stage, of 12 flybys only the half will have visibility from Malargüe during the CA with the moon, offering the possibility to collect three-way data with LLAMA. In this work, the technique has been applied only on these arcs, when the impact of TDMC noise suppression on the gravity analysis is maximum.

According to last trajectory kernel, the most promising flybys for measuring the tidal deformation of the moon are C1, C11 and C12. In fact, differently from the other flybys (all sharing the same Callisto's true anomaly), these three offer a well distributed sampling of the tidal phenomenon throughout Callisto's orbit around Jupiter.

The results on the estimated parameters are summarized in Tab. 3, highlighting enhancements of 30% on the *GM* estimate, 38% on J_2 and 40% on k_2.

Furthermore, Cappuccio et al. [12] shows that, by losing even only one of these three flybys for any issue that could occur at the GS or at the SC-side, the possibility to unveil the eventual presence of a subsurface ocean is compromised. Therefore, TDMC acquires another crucial role for the mission, offering a unique backup on this vital data and thus granting the success of the experiments even under unfavorable weather conditions at the transmitting antenna.

Table 3. Callisto's *GM*, J_2 and k_2 formal uncertainties obtained for 3GM simulations. The formal accuracies achieved with the reference 2-way tracking configuration (top) and TDMC with LLAMA on Malargüe passages (bottom) are compared.

GM	J_2	k_2
Two-way (DSA 3):		
1.87E-4	7.60E-8	8.39E-2
TDMC (DSA 3 / LLAMA):		
1.31E-4	4.74E-8	5.07E-2

6. Conclusions

In this work, the potential results obtained with the implementation of a multi-station tracking configuration for the reduction of Doppler noise on BepiColombo's MORE and JUICE's 3GM radio science experiments are presented.

For the gravity experiment of BepiColombo this translates in an overall reduction of the RMS of the residuals that produces a ~1.7 gain factor on the estimate

parameters, that is a level of amelioration comparable to the one achievable with the 2-year extended mission [10].

Sharing most of MORE's fundamental concepts (section 3.1), JUICE's radio science experiment 3GM equally benefits of the potential TDMC noise suppression effects. The analysis conducted shows that, if applied on selected flybys which have a pivotal rule in the gravity experiment, a ~40% reduction on the overall estimate of Callisto's geophysical parameters is possible. Of particular interest are the consequences on the estimate of the tidal Love number k_2, and its implications on the investigation of Callisto's interior structure. Indeed, a σ_{k_2}<0.07, as the one granted by TDMC, should be sufficient for inferring the possible presence of a liquid ocean beneath the moon's icy shell.

Acknowledgements

The authors would like to thank the colleagues of the Radio Science Laboratory of Sapienza University for the fruitful discussions and valuable advices.

References

[1] W. Riley and D. A. Howe, "Handbook of Frequency Stability Analysis," *NIST SP,* no. 1065, 2008.

[2] S. W. Asmar, J. W. Armstrong, L. Iess and P. Tortora, "Spacecraft Doppler Tracking: Noise budget and accuracy achievable in precision radio science observations," *Radio Science,* vol. 40, 2005.

[3] L. Iess, M. Di Benedetto, N. James, M. Mercolino, S. Lorenzo and T. Paolo, "Astra: Interdisciplinary study on enhancement of the end-to-end accuracy for spacecraft tracking techniques," *Acta Astronautica,* vol. 94, no. 2, pp. 699-707, 2014.

[4] V. Giordano, C. Fluhr, S. Grop and B. Dubois, "Tests of Sapphire Crystals Manufactured With Different Growth Processes for Ultra-Stable Microwave Oscillators," *IEEE Trans. Microw. Theory Tech,* vol. 64, no. 1, pp. 78-85, 2015.

[5] J. W. Armstrong, F. B. Estabrook, S. W. Asmar, L. Iess and P. Tortora, "Reducing antenna mechanical noise in precision spacecraft tracking," *Radio Science,* vol. 43, 2008.

[6] A. Greve and J. Mangum, "Mechanical Measurements of the ALMA Prototype Antennas," *IEEE Antennas Propag. Mag.,* vol. 50, no. 2, pp. 66-80, 2008.

[7] ESO, "Apex Weather Archive Query Form," [Online]. Available: http://archive.eso.org/wdb/wdb/asm/meteo_apex/form. [Accessed 2018].

[8] S. J. Keihm, "Water Vapor Radiometer Measurements of the Tropospheric Delay Fluctuations at Goldstone Over a Full Year," *TDA Progress Report,* vol. 42, no. 122, 1995.

[9] L. Imperi and L. Iess, "The determination of the post-Newtonian parameter γ during the cruise phase of BepiColombo," *Class. Quantum Grav,* vol. 34, no. 7, 2017.

[10] L. Imperi, L. Iess and M. J. Mariani, "An analysis of the geodesy and relativity experiments of BepiColombo," *Icarus,* vol. 301, pp. 9-25, 2018.

[11] F. De Tiberis, L. Simone, D. Gelfusa, R. Viola, A. Santoni, O. Cocciolillo, M. Ziarelli, F. Barletta, N. Salerno, M. Maffei and V. Nanni, "The X/X/KA-band deep space transponder for the BepiColombo mission to mercury," *Acta Astronautica,* vol. 68, pp. 591-598, 2011.

[12] P. Cappuccio, M. Di Benedetto, G. Cascioli and L. Iess, "Analysis of the 3GM gravity experiment of ESA's JUICE mission," *Advances in the Astronautical Sciences,* no. 167, pp. 3551-3561, 2018.

[13] B. D. Tapley, B. E. Schutz and G. H. Born, "Fundamentals of Orbit Determination," in *Statistical Orbit Determination*, Elsevier Academic Press, 2004, pp. 159-190.

[14] A. Milani and G. Gronchi, "Multi-Arc Strategy," in *Theory of Orbit Determination*, Cambridge University Press, 2009, pp. 311-322.

[15] E. Mazarico, A. Genova, S. Goossens, F. G. Lemoine, G. A. Neumann, M. T. Zuber, D. E. Smith and S. C. Solomon, "The gravity field, orientation, and ephemeris of Mercury from MESSENGER observations after three years in orbit," *JGR Planets,* vol. 119, no. 12, pp. 2417-2436, 2014.

[16] J. D. Anderson, R. A. Jacobson, T. P. McElrath, W. B. Moore, G. Schubert and P. C. Thomas, "Shape, Mean Radius, Gravity Field, and Interior Structure of Callisto," *Icarus,* vol. 153, no. 1, pp. 157-161, 2001.

[17] V. Notaro, M. J. Mariani, A. Di Ruscio, L. Iess, J. W. Armstrong and S. W. Asmar, "Feasibility of an innovative technique for noise reduction in spacecraft Doppler

tracking," in *2018 IEEE Aerospace Conference*, Big Sky, MT, USA, 2018.

[18] R. Notarpietro, M. Cucca and S. Bonafoni, "GNSS Signals: A Powerful Source for Atmosphere and Earth's Surface Monitoring," in *Remote Sensing of Planet Earth*, IntechOpen, 2012, pp. 172-200.